Scientific Research Publishing

International Journal of Geosciences, 2017, 8, 1080-1090
http://www.scirp.org/journal/ijg
ISSN Online: 2156-8367
ISSN Print: 2156-8359

A Study on the VLF/LF Long Term Amplitude Oscillations Associated with Frequencies 37.5 kHz and 45.9 kHz Received at Keil Longwave Monitor, Keil, Germany

Govinda Sharma[1,2*], Keshav Prasad Kandel[1,2*], Balaram Khadka[2,3], Peter Wilhelm Schnoor[4], Karan Bhatta[1,2], Basu Dev Ghimire[2,3], Aditya Singh Thapa[1,2]

[1]St. Xavier's College, Kathmandu, Nepal
[2]Nepalese Center for Research in Physical Sciences (NCRPS), Kathmandu, Nepal
[3]Department of Physics, St. Xavier's College, Kathmandu, Nepal
[4]Keil Longwave Monitor, Keil, Germany
Email: *govinhood@gmail.com, *keshavkandel5@gmail.com

How to cite this paper: Sharma, G., Kandel, K.P., Khadka, B., Schnoor, P.W., Bhatta, K., Ghimire, B.D. and Thapa, A.S. (2017) A Study on the VLF/LF Long Term Amplitude Oscillations Associated with Frequencies 37.5 kHz and 45.9 kHz Received at Keil Longwave Monitor, Keil, Germany. *International Journal of Geosciences*, **8**, 1080-1090.
https://doi.org/10.4236/ijg.2017.89061

Received: August 13, 2017
Accepted: September 15, 2017
Published: September 18, 2017

Abstract

The middle and upper atmosphere of Earth displays many large-scale oscillations in several parameters. Of these oscillations, Atmospheric Oscillation (AO) and Semi-annual Oscillation (SAO) are prominent ones. In this work, we have analyzed the Very Low Frequency/Low Frequency (VLF/LF) data from two of the transmitters of frequency 45.9 kHz at NSY, Sicily, Italy and 37.5 kHz at Grindavik, Iceland. The selected Trasmitter-Receiver Great Circle Path (TRGCP) is middle latitude which is marine in case of Grindavik TRGCP and terrestrial in case of NSY TRGCP. The VLF/LF signals are bounced back and forth from D-layer of ionosphere (altitude at ~65 km during day and ~95 km during night) in Earth-ionospheric waveguide. This infers the presence of atmospheric oscillations as a consequence of change in ionization and recombination rates. Many works related to AO and SAO are mostly done only for equatorial region of the ionosphere and authors have reported the elegant dominancy of AO and SAO in the VLF/LF amplitude pattern over years. To our surprise, in our work it is seen that not only AO and SAO but also other oscillations are necessary to model the oscillation pattern of middle latitude ionosphere.

Keywords

VLF/LF, D-Layer, SAO, AO, TRGCP, NSY, Grindavik

1. Introduction

The Earth's middle and upper atmosphere (above 20 km from the surface of the earth) mainly implies stratosphere, mesosphere and thermosphere. This region reveals several dominant large-scale oscillations in many measured parameters. These dynamic oscillations are in fact the main features of these regions. These oscillations can be found at all latitudes, from the Equator to high latitudes. Two of these oscillations are the semi-annual oscillation (SAO) and annual oscillation (AO) are detected in neutral atmospheric measures. For example, the SAO in wind fields of mesosphere-lower thermosphere (MLT) are observed in number studies [1]-[6]. The important oscillation is SAO occurring mainly at equator in the regions of stratosphere and mesosphere [7]. The AO of temperature and wind has been a matter of study since 1960s majorly in many works [8] [9]. AO is found to be prominent mainly in high latitudes. The amplitudes of those oscillations are higher in mesosphere than in stratosphere. The cause of these oscillations in stratosphere is due to solar heating and in mesosphere is believed to be generated by the filtering of gravity waves [10]. SAO is more dominant in nighttime amplitudes of VLF in some cases [11]. The author Israel Silber reports the cause to be the transportation of NO_X molecule from lower levels of thermosphere, resulting in ionization and creation of free electrons in nighttime D-regions, showing SAO Oscillations. As not many works are done for AO and SAO oscillations of VLF/LF, this work of ours is of great importance.

The D-layer of the ionosphere which lies at altitudes of ~80 - 95 km during nighttime and lowers down to ~60 km during day time due to solar radiation, is crucial. The chemistry and formation of D-layer infer to be neutral environment and therefore, experience oscillations [12] [13]. To study this region was a tedious and difficult job till the discovery of remote sensing. Among remote sensing also, the use of Very low frequency (VLF/LF) radio waves (3 - 300 kHz) is more prominent because it is effectively reflected by the D-region of the ionosphere. These waves, generated both in natural and artificial manners, reflect off back and forth in the Earth-ionosphere waveguide to long distance and this way, revealing to us the secrets of important features of ionosphere.

2. Transmitters and Receivers

Receiver is located at Keil, Germany where narrow band (NB) VLF/LF signals were recorded. The VLF/LF recording system of Kiel Longwave Monitor (KLM) consists of mainly three parts; one receiving antenna, one receiver/amplifier, and one computer. A Thin-Client computer is used in the setup of KLM along with an identical ferrite loop antennae, running at a constant location in a constant direction. The antenna nulls at 50 and 230 degrees. The receivers, built in 2009, are broadband of 10 - 90 kHz running 90 Fast Fourier Transforms (FFT) per second.

Each datum used in this case was a one minute spectrum was an average from approximately 5000 raw spectra. The Kiel Longwave Monitor records the VLF/LF spectrum between 10 and 96 kHz by means of two receivers running at 6 km of distance. The H-field probe has a location of 54˚23'46"N 10˚03'13"E whereas the E-field has a location of Loc: 54˚22'24"N 10˚08'15"E. The receiver panel is shown in Figure 1.

The description of the two transmitters is given in Table 1. Sites are estimated from own bearings and various sources. Bearings and distances refer to Kiel, North Germany.

These transmitters were selected because of their high radiated power, fixed frequency band and their continuous operation. The data were almost complete with high signal-to-noise ratio. The NSY transmitter's signal of 45.9 kHz and Grindavik's signal of 37.5 kHz were recorded at the years 2010-2014. We extracted two data sets of the average amplitude during the midday and midnight hours from each time series of transmitter-receiver amplitudes. The variation in recorded amplitude and phase of VLF/LF implies the changes of the D region along the path. The path is named here as Transmitter-Receiver Great Circle Path abbreviated as TRGCP. Figure 2 displays the clear pathway between our receiver and two transmitters.

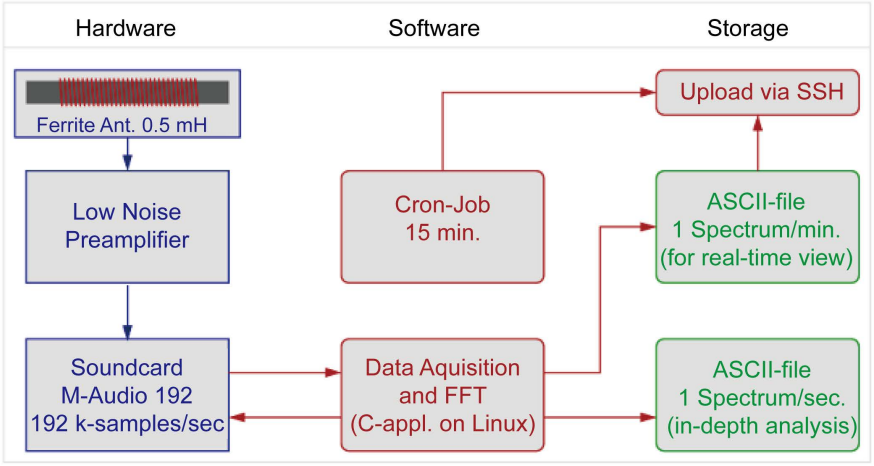

Figure 1. Block Diagram of Kiel Longwave Monitor where Ferrite Antennae receives the VLF/LF signals, amplifies and processed to obtain ASCII file finally minute average data and second average data. It uploads the data into web via SSH. The blue arrow represents the series of hardware procedures and red arrow represents the procedures originating from Software used. Hardware, Software and Storage are distinguished with Blue, Red and Green Colour.

Table 1. Description of Transmitters.

Frequency [kHz]	Parameters		
	Place	Geo-coordinates	Distance/Bearing
45.90	NSY, Niscemi, Navy, Italy	37˚07'N14˚26'E	1928 km/171˚
37.50	Grindavik, Navy, Iceland	63˚51'N22˚28'W	2119 km/314˚

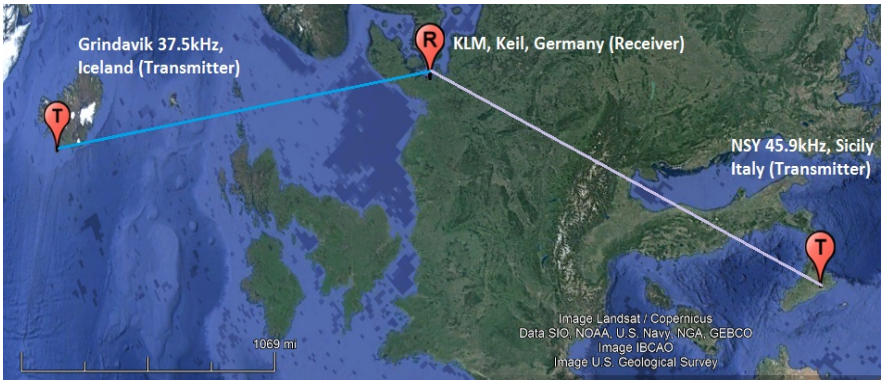

Figure 2. The transmitters are located in Grindavik, Iceland 37.5 kHz (TRGCP shown in blue line) and NSY, Sicily 45.9 kHz, Italy (TRGCP show in light blue) connected to receiver in Keil, Germany.

3. Methodology

As each datum used in this case was a one minute spectrum was an average fromapproximately 5000 raw spectra. The graph of daily data clearly shows two distinct points during terminator times (around sunrise and sunset) when the amplitude is minimum. During the day and night excluding the terminator times, the VLF/LF data is less variable. Therefore, the effect of terminator times is essential to be removed. As the sunrise and sunset time varies in different seasons, the terminator time effect varies with the time (or season) of year. For example, the VLF/LF day data is significantly less in January, gradually increases up to June-July and then gradually decreases. This is because the daytime and nighttime length varies throughout the year. The terminator time therefore varies from 1 hr - 3 hrs. We sketched graphs of each month of five consecutive years and removed the terminator time effect in ORIGIN. This also removed the possibilities of Tidal oscillations to much extent.

We found the average data marked the two sigma lines and eliminated all those data crossing two sigma lines to wipe out possible anomalies in data. The anomalous data might be due to various factors including lightning, solar flares, storms, auroras, tidal oscillations and due to unpredictable shut down of either transmitter or receiver. Moreover, we used MATLAB coding for doing the running average of hourly data to obtain 24 values for the day. The purpose of running average is to smooth out the data and give more precise mean. Repeating the procedure of running average, henceforth, we got daily one datum, a total of around 1800 data for 5 years. These data are plotted in order to obtain the desired raw oscillations. Due to insufficient data of 11 years, which comprises a solar cycle, we decided to do least square (LS) harmonic fitting to obtain periodic signals [11]. The equation of fitting is as follows in Equation (1).

$$\begin{aligned} A_{fit(t)} &= A_0 + St + A_{SAO}\cos\left[2\pi\left(t - t_{SAO}\right)/182.625\right] \\ &+ A_{AO}\cos\left[2\pi\left(t - t_{AO}\right)/365.25\right] \end{aligned} \quad (1)$$

where A_{fit} is the fitted curve; t represents the time steps (in days); A_0 is the mean amplitude (which varies in our case); S is the trend coefficient; A_{SAO} and A_{AO} are the fitted SAO and AO amplitudes, respectively; and t_{SAO} (t_{AO}) represents the SAO (AO) maximum time of year. The nonlinear least square fitting method is applied to determine the unknown variables. Using this procedure, the SAO and AO are derived along with other inter-annual variations.

Later, we performed spectral analysis called Lomb-Scargle Spectral Analysis to check and compare the dominancy of either of these oscillations AO and SAO. We could not use Fast Fourier Transforms (FFTs) as our data were unevenly sampled due to transmitter off-times, receiver malfunctions and so on. LS periodogram, on the other hand, allows the spectral analysis of unevenly sampled data [14]. FFTs requires uniform time steps between samples. Therefore, we have analyzed the midday and midnight 1 h mean data using the Lomb-Scargle (LS) periodogram [15], which results in spectral power of the data at user-determined frequencies (and, hence, time periods).

4. Results

The midday and midnight 1 h mean 30-day running-average time series for the Grindavik and NSY TRGCP deviation from the mean amplitude (of the entire time series) are shown in **Figure 3** and **Figure 4** (black solid curves). As can be seen, all the time series exhibit a strong oscillatory behavior, with higher amplitudes in the midday data than in the midnight data. However, the midday data Grindavik TRGCP show a dominant oscillation with longer time periods than the midnight data and midnight data NSY TRGCP show a dominant oscillation with longer time period than the midday. Moreover, the trends in all cases are analyzed **Table 2**.

A trend can be seen in time series, positive in all-time series except in the midday of Grindavik TRGCP, where it was negatively correlated with its coefficient −0.00082. However, there was positive correlation of VLF amplitude with solar activity in NSY TRGCP. It confirmed the work by Thomson and Clilverd (2000) that trend is a result of solar activity [16]. This was not true, however, in case of Grindavik TRGCP.

Harmonic fits were made using a least-squares method over all of the data

Table 2. Trend and correlation coefficient.

Frequency (kHz)	Table Column Head		
	Time of the Day	Trend Coefficient	Correlation Coefficient
37.5	Day	−0.00082	0.34
37.5	Night	0.000474	0.21
45.9	Day	0.000615	0.22
45.9	Night	0.000474	0.17

a. Sample of a Table footnote (*Table footnote is dispensable*).

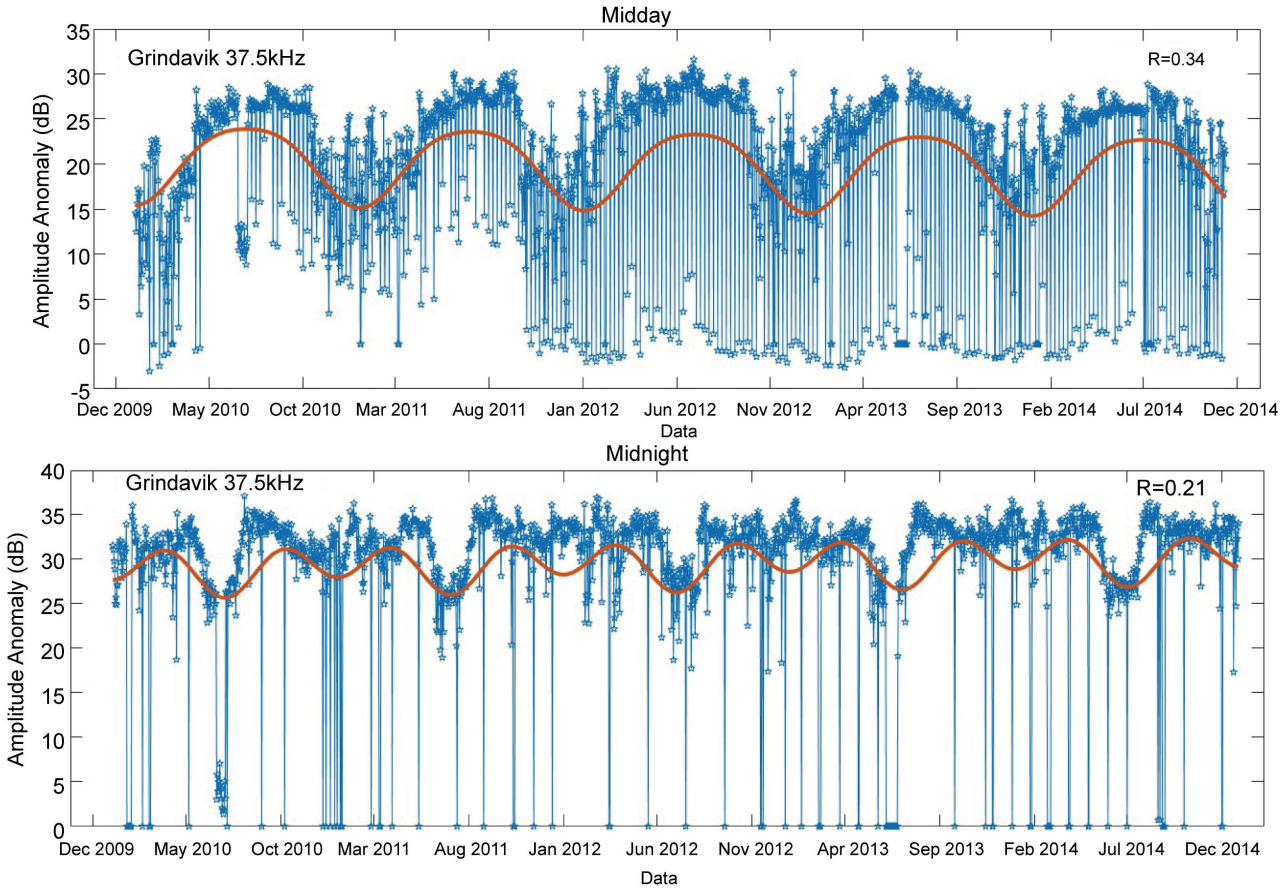

Figure 3. Midday (top panel) and midnight (bottom panel) 1 h mean 30-day running-average time series of Grindavik transmitter-receiver TRGCP deviation from the mean amplitude (solid red curves). The dashed red curves show the combination of the SAO, AO, and linear fit to the data time series (see Equation (1)). A Pearson's correlation coefficient between the red and blue curves is shown at the top right of each panel.

points. The fitted curves are shown as dashed red. Pearson's correlation coefficients between the time series and the fitted curves were calculated and are shown at the top right of each panel. The correlation coefficients calculated in our case, are significantly low. These span from 0.17 to 0.34. For example, correlation was found to be more in midday (0.34 for Grindavik TRGCP & 0.22 for NSY TRGCP) than in midnight (0.21 for Grindavik TRGCP & 0.17 for NSY TRGCP). This implies that raw data can explain the long-term variability for midday better than midnight.

The appropriate reasoning behind correlation coefficients to be low is explained well in next section that deals with Long-scargle periodogram analysis. We suspect the presence of many other oscillations (other than AO and SAO) as well, irrespective of our considerations (which are only for AO and SAO). **Figure 5** shows the LS periodogram of the midday Grindavik TRGCP (top panel) NSY TRGCP (bottom panel) 1 h mean VLF amplitude anomalies, with arbitrary power units (as a result of the LS periodogram procedure). The dashed red line denotes 95% confidence, which was calculated.

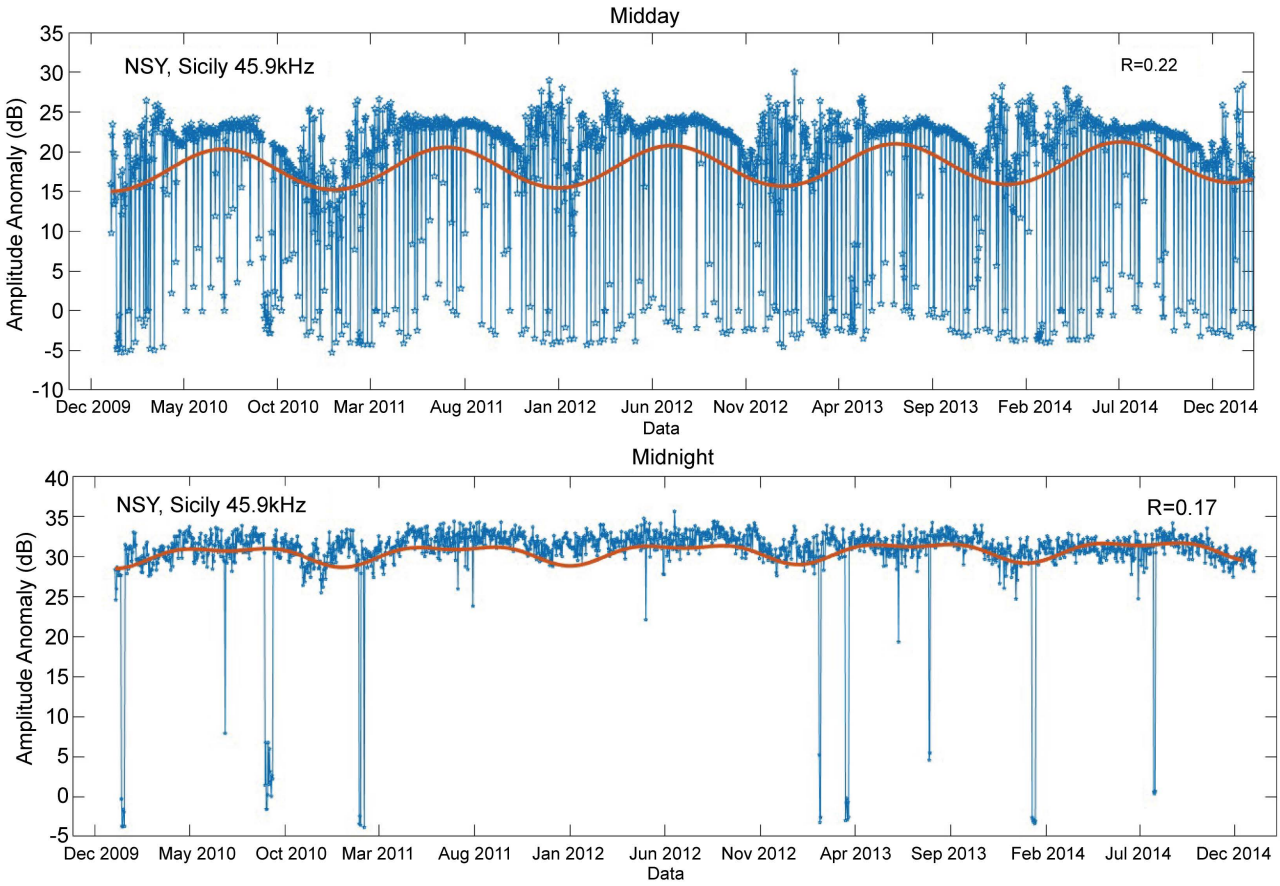

Figure 4. Midday (top panel) and midnight (bottom panel) 1 h mean 30-day running-average time series of NSY transmitter-receiver TRGCP deviation from the mean amplitude (solid red curves). The dashed red curves show the combination of the SAO, AO, and linear fit to the data time series (see Equation (1)). A Pearson's correlation coefficient between the red and blue curves is shown at the top right of each panel.

The appropriate reasoning behind correlation coefficients to be low is explained well in next section that deals with Long-scargle periodogram analysis. We suspect the presence of many other oscillations (other than AO and SAO) as well, irrespective of our considerations (which are only for AO and SAO). **Figure 5** shows the LS periodogram of the midday Grindavik TRGCP (top panel) NSY TRGCP (bottom panel) 1 h mean VLF amplitude anomalies, with arbitrary power units (as a result of the LS periodogram procedure). The dashed red line denotes 95 % confidence, which was calculated. Examination of both the LS periodogram daytime confirms that the AO at ~365 days (0.0027 day^{-1}) is most dominant and significant oscillation during the daytime. The second peak of the periodogram is of ~180 days (0.0054 day^{-1}). This peak is called SAO. Although observed to be distinct during midday in Grindavik TRGCP, the oscillation was out of sight in NSY TRGCP because it doesn't cross the 95% confidence interval (although it is there). The peaks having enough strength to cross over the 95% interval are regarded as distinct oscillations and other than these which have little influence are termed as Secondary peaks. All the secondary peaks are discarded in the theoretical calculations too.

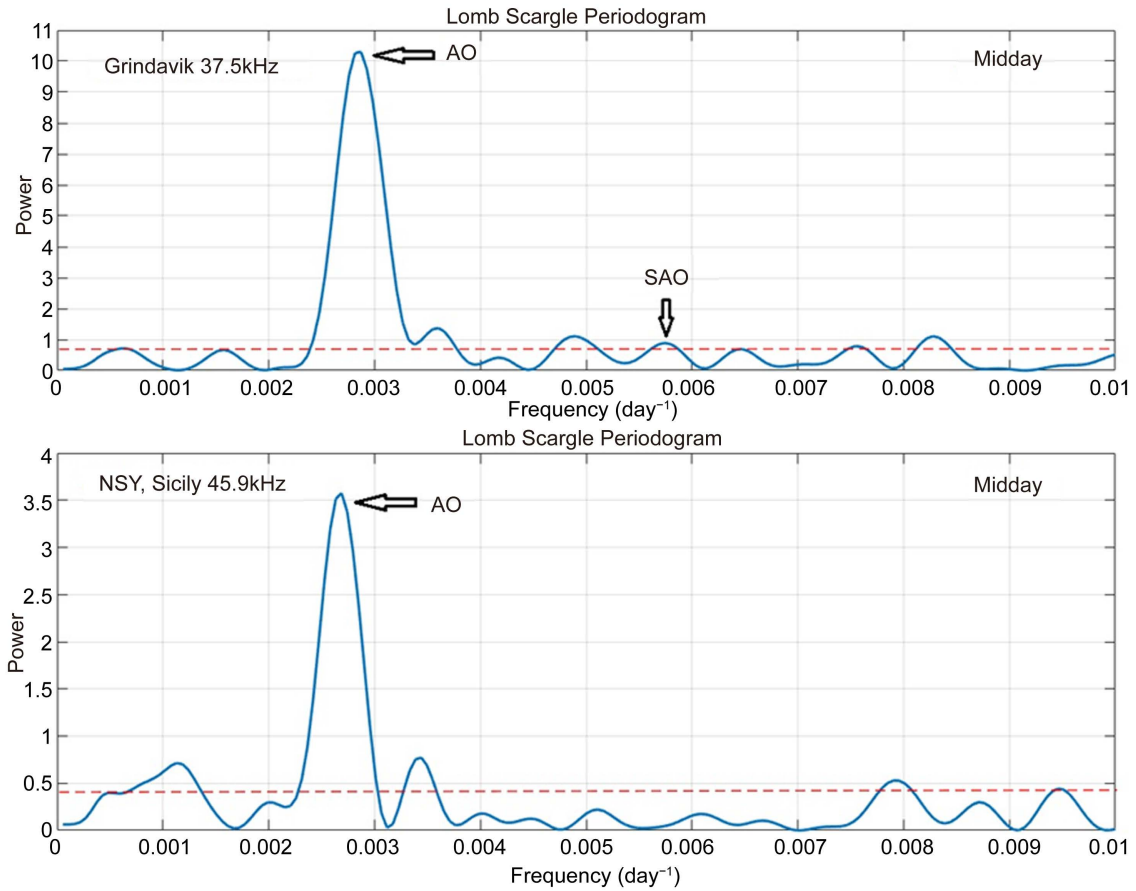

Figure 5. Lomb-Scargle periodogram of the midday Grindavik TRGCP (top) and NSY TRGCP (bottom) 1 h mean VLF/LF amplitude anomalies in arbitrary power units. The dashed red line denotes the 95% confidence level.

Similar dominancy of AO over SAO is observed during midnight in NSY TRGCP as shown in the **Figure 6**. However, during midnight, SAO was seen more dominant over AO in Grindavik TRGCP. This dominant nature of SAO was shown in the work of Silber *et al*. Other than the AO and SAO, there were plenty of other peaks crossing the threshold confidence intervals, which are not taken into account in Equation (1) and therefore correlation was significantly low. Most no. of peaks are seen in midnight data. For example, in Grindavik TRGCP, peaks are seen at time periods of 111, 133, 151 and 217 days & in NSY TRGCP, there is one prominent heap and many other secondary peaks whose combined effect can be significant. Such primary peaks other than AO and SAO were also present during daytime. Some of these oscillations might be higher harmonics of the SAO, but it is not possible to explain them at the moment, leaving this topic for future studies. Many such oscillations might be an indication towards quasi-biennial oscillation (QBO) affect. The probable signature of the AO seen in this periodogram is also statistically significant, peaking at 365 days.

Even though we tried our best, certain limitations were there. The reason for low correlation might be due the undesired and unexpected shut down of either

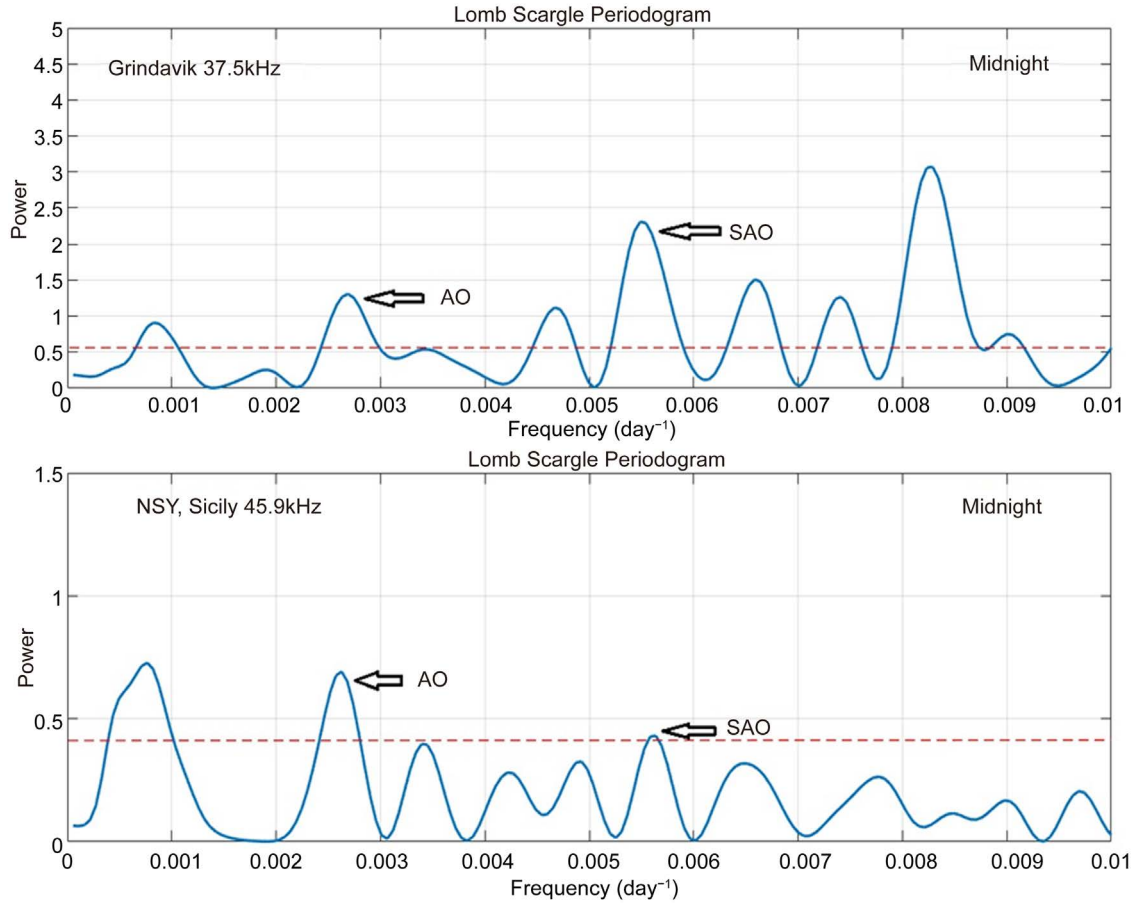

Figure 6. Lomb-Scargle periodogram of the midnight Grindavik TRGCP (top) and NSY TRGCP (bottom) 1 h mean VLF/LF amplitude anomalies in arbitrary power units. The dashed red line denotes the 95% confidence level.

transmitter and receiver and presence of unwanted noise. This was completely not in our hands. In such circumstances, there is almost no correlation between observed and expected amplitudes, which affects the overall correlation for total data. Gradual deterioration of transmitter and receiver hardware has not been accounted; they change the signal to noise ratio. Moreover, we only studied data of only 5 years; a data of 11 years comprising a solar cycle would give better results. We analyzed only two frequencies; more the number of frequencies, better would be the results.

Our study could not account for the physical cause of dominancy of AO over SAO in three cases which could be a subject for future studies. The cause for SAO dominancy over AO during midnight in Grindavik TRGCP was explained by Silber *et al.* [11].

5. Conclusions

We examined five years of VLF NB data received in North-East hemisphere (NSY TRGCP) and North-west hemisphere (Grindavik TRGCP), during midday and midnight hours. The analysis shows that the AO dominates midday VLF/LF amplitudes, and the SAO is the strongest oscillation during the midnight in

Grindavik TRGCP. The correlation coefficient between the moving averaged raw data and harmonic best fit, was found to be significantly low. This might be because of presence of other primary peaks present (of unknown origin other that SAO and AO), which were not included in our least square best fit equation. Other than this, the continuous working of transmitter and receiver system might have been obstructed because of undesired shut down affecting the correlation of data as a whole.

VLF/LF signal studies are an important tool for understanding the D region of the ionosphere, being low-cost and having high temporal resolution and potentially high spatial resolution (by using numerous receivers at many different locations). Therefore, propagation models should take this oscillation into consideration, in order to acquire better and more precise results, particularly over long time periods.

Acknowledgements

The authors thank Prof. Craig J. Rodger (University of Otago) and Dr. Israel Silber (Tel Aviv University) for useful discussion through E-mail regarding the work; Mr. Peter Wilhelm Schnoor (Head at Keil Longwave Monitor) for providing data.

References

[1] Gregory, J.B. and Manson, A.H. (1975) Winds and Wave Motions to 110 km at Mid-Latitudes. II. Mean Winds at 52°N, 1969-73. *Journal of the Atmospheric Sciences*, **32**, 1667-1675. https://doi.org/10.1175/1520-0469(1975)032<1667:WAWMTK>2.0.CO;2

[2] Lysenko, I.A., Portnyagin, Y.I., Fakhrutdinova, A.N., Ishmuratov, R.A., Manson, A.H. and Meek, C.E. (1994) Wind Regime at 80-110 km at Mid-Latitudes of the Northern Hemisphere. *Journal of Atmospheric and Terrestrial Physics*, **56**, 31-42. https://doi.org/10.1016/0021-9169(94)90173-2

[3] Groves, G.V. (1972) Annual and Semi-Annual Zonal Wind Components and Corresponding Temperature and Density Variations, 60-130 km. *Planetary and Space Science*, **20**, 2099-2112.https://doi.org/10.1016/0032-0633(72)90066-9

[4] Huang, F.T., Mayr, H.G., Reber, C.A., Russell, J.M., Mlynczak, M. and Mengel, J.G. (2006) Stratospheric and Mesospheric Temperature Variations for the Quasi-Biennial and Semiannual (QBO and SAO) Oscillations Based on Measurements from SABER (TIMED) and MLS (UARS). *Annales Geophysicae*, **24**, 2131-2149. https://doi.org/10.5194/angeo-24-2131-2006

[5] Taylor, M.J., Taori, A.K., Hatch, D.R., Liu, H.L. and Roble, R.G. (2005) Characterization of the Semi-Annual-Oscillation in Mesospheric Temperatures at Low-Latitudes. *Advances in Space Research*, **35**, 2037-2043. https://doi.org/10.1016/j.asr.2005.05.111

[6] Shepherd, M.G., Liu, G. and Shepherd, G.G. (2006) Mesospheric Semiannual Oscillation in Temperature and Nightglow Emission. *Journal of Atmospheric and Solar-Terrestrial Physics*, **68**, 379-389. https://doi.org/10.1016/j.jastp.2005.02.029

[7] Remsberg, E.E., Bhatt, P.P. and Deaver, L.E. (2002) Seasonal and Longer-Term Variations in Middle Atmosphere Temperature from HALOE on UARS. *Journal of Geophysical Research: Atmospheres*, **107**, No. D19. http://doi/10.1029/2001JD001366

[8] Swinbank, R. and Ortland, D.A. (2003) Compilation of Wind Data for the Upper Atmosphere Research Satellite (UARS) Reference Atmosphere Project. *Journal of Geophysical Research: Atmospheres*, **108**, No. D19. http://doi/10.1029/2002JD003135

[9] Fleming, E.L., Chandra, S., Barnett, J.J. and Corney, M. (1990) Zonal Mean Temperature, Pressure, Zonal Wind and Geopotential Height as Functions of Latitude. *Advances in Space Research*, **10**, 11-59. https://doi.org/10.1016/0273-1177(90)90386-E

[10] Mayr, H.G., Mengel, J.G., Chan, K.L. and Huang, F.T. (2010) Middle Atmosphere Dynamics with Gravity Wave Interactions in the Numerical Spectral Model: Zonal-Mean Variations. *Journal of Atmospheric and Solar-Terrestrial Physics*, **72**, 807-828. https://doi.org/10.1016/j.jastp.2010.03.018

[11] Silber, I., Price, C. and Rodger, C.J. (2016) Semi-Annual Oscillation (SAO) of the Nighttime Ionospheric D Region as Detected through Ground-Based VLF Receivers. *Atmospheric Chemistry and Physics*, **16**, 3279-3288. https://doi.org/10.5194/acp-16-3279-2016

[12] Silber, I., Price, C., Rodger, C.J. and Haldoupis, C. (2013) Links between Mesopause Temperatures and Ground-Based VLF Narrowband Radio Signals. *Journal of Geophysical Research*: *Atmospheres*, **118**, 4244-4255. https://doi.org/10.1002/jgrd.50379

[13] Marshall, R.A. and Snively, J.B. (2014) Very Low Frequency Subionospheric Remote Sensing of Thunderstorm-Driven Acoustic Waves in the Lower Ionosphere. *Journal of Geophysical Research*: *Atmospheres*, **119**, 5037-5045. https://doi.org/10.1002/2014JD021594

[14] Press, W.H. and Rybicki, G.B. (1989) Fast Algorithm for Spectral Analysis of Unevenly Sampled Data. *The Astrophysical Journal*, **338**, 277-280. https://doi.org/10.1086/167197

[15] Lomb, N.R. (1976) Least-Squares Frequency Analysis of Unequally Spaced Data. *Astrophysics and Space Science*, **39**, 447-462. https://doi.org/10.1007/BF00648343

[16] Thomson, N.R. and Clilverd, M.A. (2000) Solar Cycle Changes in Daytime VLF Subionospheric Attenuation. *Journal of Atmospheric and Solar-Terrestrial Physics*, **62**, 601-608.